ELSEVIER

Quaternary Science Reviews 23 (2004) 935–945

QSR

Palaeoclimatic interpretation of high-resolution oxygen isotope profiles derived from annually laminated speleothems from Southern Oman

Dominik Fleitmann[a,*], Stephen J. Burns[b], Ulrich Neff[c], Manfred Mudelsee[d], Augusto Mangini[e], Albert Matter[a]

[a] *Institute of Geological Sciences, University of Bern, Baltzerstrasse 1-3, Bern 3012, Switzerland*
[b] *Department of Geosciences, Morrill Science Center, University of Massachusetts, Amherst MA 01002 USA*
[c] *Heidelberg Academy of Sciences, Im Neuenheimer Feld 229, Heidelberg 69120, Germany*
[d] *Institute of Meteorology, University of Leipzig, Stephanstr. 3, Leipzig 04103, Germany*
[e] *Heidelberg Academy of Sciences, Im Neuenheimer Feld 229, Heidelberg 69120, Germany*

Received 3 February 2003; accepted 13 June 2003

Abstract

High-resolution stable isotope profiles of three contemporaneously deposited stalagmites from a shallow cave in Southern Oman provide an annually resolved record of Indian Ocean monsoon rainfall variability for the past 780 years. Uranium-series age dating and counts of annual growth bands enable an excellent age calibration. Although modern speleothems do not grow in perfect isotopic equilibrium, oxygen isotope ratios ($\delta^{18}O$) are a proxy for the amount of monsoon rainfall. This is supported by the statistically significant correlation between $\delta^{18}O$ and the thickness of annual bands, whereas $\delta^{18}O$ is inversely correlated with annual band thickness. Additionally, overlapping $\delta^{18}O$ profiles are very similar in pattern and range, indicating that sample specific noise did not blur the climatic signal. The longest oxygen isotope profile, derived from stalagmite S3, clearly shows the transition at ~1320 AD from a generally wetter Medieval Warm Period to a drier Little Ice Age that lasted from approximately AD 1320–1660 in Southern Oman. The decrease in monsoon rainfall since the 1960s is also obvious in meteorological records from Northern Africa and India, indicating that our speleothem-based rainfall records do not only reflect local monsoon rainfall variability.

1. Introduction

Countries located in the Indian monsoon domain are densely populated with their economy depending to a large extent on rain-fed agriculture. Major departures from normal monsoonal rainfall cause serious famines and migration and politic instability. To better predict catastrophic monsoon failures, the monsoon dynamics and its linkages to other climate phenomena, such as the El Niño-Southern Oscillation (ENSO) in the Pacific Ocean and Eurasian snow cover, must be well understood. Our current knowledge of the Indian monsoon dynamics remains limited, mainly due to the lack of high-resolution and long-term monsoon records. The longest instrumental data of monsoon rainfall variability cover the last 150 years (Parthasarathy et al., 1994) and are, thus, too short to fully reveal monsoon variability on century-long time scales. On longer time scales only a few high-resolution geographically widely distributed paleomonsoon records, based on ice cores (Thompson et al., 1997), tree-rings (Bräunig, 1994) and marine sediments (von Rad et al., 1999; Agnihotri et al., 2002; Anderson et al., 2002), are currently available. Even more acute is the lack of information on the Arabian Peninsula and in Northern Africa. A source for information of Indian Ocean monsoon variability is annually laminated speleothems, such as stalagmites and flowstones, forming in caves in Southern Oman where still a monsoon-type climate exists (Burns et al., 2002; Fleitmann et al., 2003). To date, most speleothem-based palaeoclimate reconstructions rely either upon oxygen ($\delta^{18}O$) isotopic measurements of speleothem calcite or upon thickness of annual

*Corresponding author. Stanford University, 325 Braun Hall (bldg 320), Stanford, CA 94305-2115, USA.
E-mail address: fleitman@pangea.stanford.edu (D. Fleitmann).

0277-3791/$ - see front matter © 2004 Elsevier Ltd. All rights reserved.
doi:10.1016/j.quascirev.2003.06.019

growth bands. The importance of both proxies as palaeoclimate variables is described hereinafter. When speleothems are deposited under conditions of isotopic equilibrium, $\delta^{18}O$ of speleothem calcite reflect either variations in $\delta^{18}O$ of the seepage water forming the speleothem and/or variations in cave air temperature. In the first case, the oxygen isotopic composition of the seepage water from which the speleothems are formed reflects the isotopic composition of mean annual rainfall (Yonge et al., 1985). In the second case, the temperature-dependent fractionation of $\delta^{18}O$ between water and calcite (−0.24‰ per 1°C; O'Neil et al., 1969) can be used to reconstruct cave air temperatures (e.g. Lauritzen and Lundberg, 1999), which relates in many caves to mean annual surface air temperature (Wigley and Brown, 1976). However, in most caves the temperature-controlled variations in $\delta^{18}O$ are obscured by changes in $\delta^{18}O$ of the seepage water and surface precipitation, respectively. Generally, changes in $\delta^{18}O$ of rainfall result from a variety of factors, including: (1) changes in $\delta^{18}O$ of the oceanic source region (important on glacial–interglacial time scales), (2) changes in moisture sources or storm tracks, (3) changes in the proportion of rainfall (e.g. winter/summer rainfall), (4) air temperature, (5) amount of rainfall, and (6) evaporation. Particularly evaporation can alter the original oxygen isotopic composition of rainfall and seepage water, respectively (e.g. Bar-Matthews et al., 1996) when the cave is located in an arid or semi-arid regions, such as Southern Oman. To rule out the importance of evaporation processes, the oxygen isotopic composition of water along the pathway from precipitation to speleothem calcite must be traced. The knowledge of the principal controls on the oxygen isotopic composition of present-day stalagmites is essential before $\delta^{18}O$ values of fossil stalagmites can be interpreted correctly in terms of palaeoclimate variability.

The thickness of annual growth bands in stalagmites is also a frequently used speleothem climate proxy, because band thickness is controlled by the drip rate, which relates to surface precipitation (Baker et al., 1993; Genty and Quinif, 1996; Holmgren et al., 1999; Qin et al., 1999). Qin et al. (1999) suggested that the thickness of annual growth bands is a proxy for the amount of drip water and surface precipitation respectively when the cave has a simple hydrological connection to the surface (thin overburden bedrock thickness). Furthermore, the stalagmite should have a columnar shape indicating that calcite precipitated at the top and no stalactite as a drip source.

Before speleothem-based time series can be used for palaeoclimate studies the following fundamental questions must be answered:

1. Are the stalagmites deposited in isotopic equilibrium with the cave waters?
2. Is the oxygen isotopic composition of speleothem calcite mainly controlled by the oxygen isotopic composition of rainfall or by air temperature?
3. Do multiple proxies, in this case $\delta^{18}O$ and annual band thickness, relate to the same climate variable?
4. Are oxygen isotope profiles of individual stalagmites reproducible?
5. Do the time series reflect local or regional climate variability?

In this paper, we present high-resolution stable isotope profiles derived from three contemporaneously deposited annually laminated stalagmites from Kahf Defore located in Southern Oman. In addition, we have sampled precipitation, cave drip waters and actively growing stalagmites to study the active water-carbonate system and to test for isotopic equilibrium. By comparing $\delta^{18}O$ and thickness of annual bands of contemporaneously deposited stalagmites we test whether both proxies relate to the same climatic variable. To date speleothem studies combining both proxies at high-resolution are extremely rare. Finally, we compare our records with meteorological observations form the surrounding areas to validate and to put our palaeoclimate reconstructions into a broader context.

2. Site location and modern climatology

Kahf Defore (17°07′N, 54°05′E; ~150 m above sea level) is located at the foothills of the Dhofar Mountains in the extreme SW of Oman (Fig. 1a and b). The cave is approximately 45 m long and has a narrow entrance (Fig. 1c). The thickness of the overlying bedrock, a karstic Eocene limestone of the Umm er Rhaduma formation varies between 15 and 20 m. Cave air temperature of 25.5°C at the sampling location closely reflects the mean air temperature of 25.7°C station at Salalah airport (1942–1998). Relative humidity (rH) in the small chamber at the end of Kahf Defore varies between 91.6% (November 1998) and 98% (August 1999). Only a few locations with dripping water were found in Kahf Defore, and drip rates were generally very slow, with less than 1 drip per minute ($dr\,min^{-1}$). The natural vegetation above the cave consists of shrubs and trees. All stalagmites were collected in a small chamber at the end of an approximately 30 m long, narrow passage (Fig. 1c).

3. The Indian monsoon in southern Oman

Today, the Indian monsoon is the most dependable source of precipitation in Southern Oman, more that 80% of total annual precipitation falls during the summer monsoon months (June, July and August).

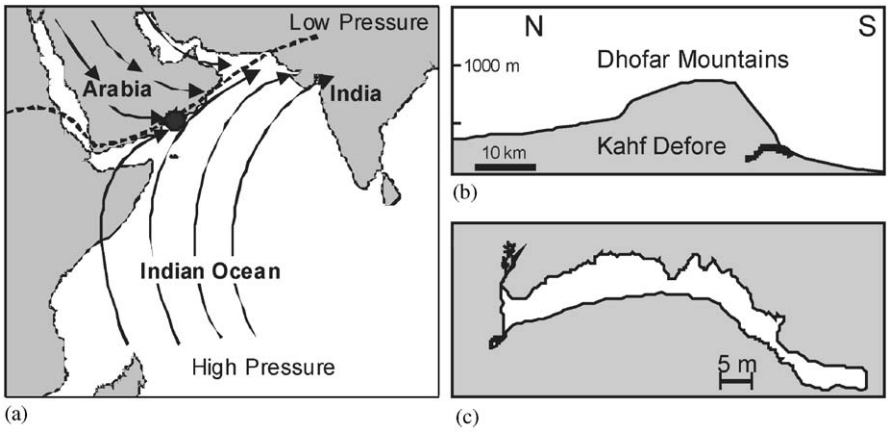

Fig. 1. (a) Location map of Kahf Defore (black circle), arrows indicate generalized modern, summer surface-wind patterns. Dashed line is the approximate position of the intertropical convergence zone (ITCZ), which today roughly marks the northern limit of summer monsoon rainfall. (b) N-S cross section through the Dhofar mountains. (c) Schematic drawing of Kahf Defore.

The Indian monsoon is driven by two fundamental mechanisms. Different sensible heating between the Asian landmass and the southern Indian Ocean results in a low atmospheric pressure cell over the Tibetan Plateau and a high atmospheric pressure cell over the southern Indian Ocean (at about 30°S; Fig. 1a). The resulting pressure gradient generates a strong low level cross equatorial airflow, which reaches its maximum intensity in June and July. The release of latent heat from condensing moisture over the Tibetan Plateau maintains and further strengthens monsoon circulation. Thus, both sensible and latent heating contribute to the land-sea temperature and pressure difference that drive the Indian summer monsoon. On annual to decadal time scales monsoon intensity is influenced by changes in internal boundary conditions, such as tropical sea surface temperatures in the Indian Ocean (Meehl and Washington, 1993; Webster et al., 1998; Burns et al., 2002) and variations in Eurasian snow cover (Barnett et al., 1988), and linkages with ENSO in the Pacific Ocean (Charles et al., 1997; Webster et al., 1998).

In Southern Oman monsoon rainfall occurs as fine drizzle, seldom exceeding more than $5\,mm\,d^{-1}$. Occult precipitation (when fog condenses on the ground and on the vegetation) is an additional source of groundwater recharge during the monsoon season. The presence of fog during the Khareef season maintains conditions of high humidity reducing evaporation. The amount of precipitation increases with altitude, varying between $150\,mm\,yr^{-1}$ at the coastal plain and more than $500\,mm\,yr^{-1}$ in the Dhofar Mountains, which reach a maximum elevation of approximately 1000 m (Fig. 1c). The mean annual air temperature at Salalah airport is 25.7°C (1942–1998) and the hottest month is June when temperature is as high as 29.0°C. With the onset of the SW-monsoon in July, the mean monthly temperature drops by approximately 3°C.

4. Sample description and methodology

All three columnar-shaped stalagmites, their lengths vary between 26 cm (S3), 7 cm (S6) and 20 cm (S9), were actively growing when sampled in November 1996 (stalagmite S3) and in August 99 (stalagmites S6 and S9) (Fig. 2a). The specimens were cut lengthwise parallel to their growth axis. The stalagmites are composed of white and grayish LMC calcite and show regular sub-millimeter lamination. No signs of secondary alternation, such as corrosion features and recrystalization, were found.

The ages of deposition were determined by U-series methods using thermal ionization mass-spectrometry. We made a total of 12 measurements for all samples. Analytical procedures for the separation and purification of thorium and uranium were as described by Ivanovich and Harmon (1993). U/Th measurements were performed on a multicollector mass spectrometer (Finnigan MAT 262 RPQ) with a double filament technique. Uranium and thorium were measured in semi-peak-jump mode and peak-jump mode, respectively. Calibration of Faraday Cup to ICM efficiency was made adopting the natural $^{238}U/^{235}U$ of 137.88. To determine the uranium and thorium concentrations, defined quantities of a $^{233}U/^{236}U$ double spike and a ^{229}Th spike were added. U/Th-ages were corrected for detritus following Ivanovich and Harmon (1993), by assuming a $^{232}Th/^{238}U$ isotope ratio of 3.8. The reproducibility of the isotope ratio of $^{234}U/^{238}U$ and the concentration of ^{232}Th of standard materials is 0.3% and 0.8% (2σ), respectively. For details about measurements of standard material refer Frank et al. (2000).

Samples (0.2–0.5 mg) for stable isotope analysis were drilled with a 0.5 mm diameter conical dentist drill. $\delta^{18}O$ and $\delta^{13}C$ isotopic composition were measured using a VG Isocarb system attached to a VG Prism II isotope

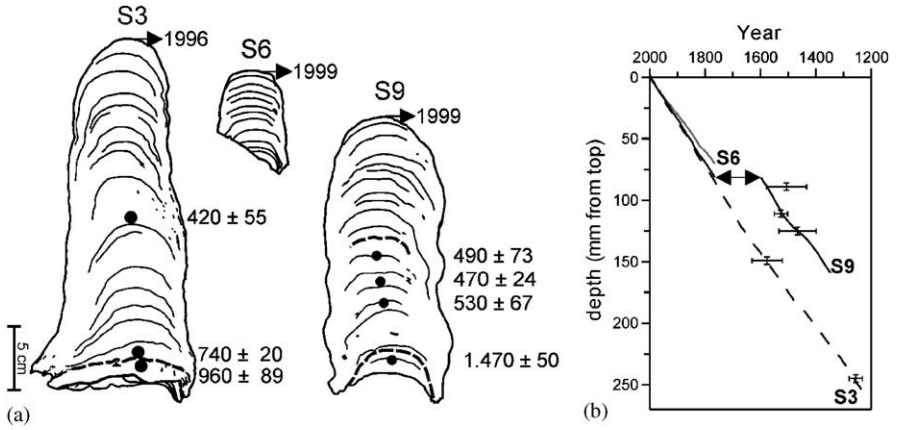

Fig. 2. (a) Schematic drawing of stalagmites S3, S6 and S9 from Kahf Defore. Black circles display the sampling location of U/Th-ages (details o U/Th-ages are shown in Table 1). Bold dashed lines (S3 and S9) indicate hiatuses. (b) Age-depth profile for stalagmites S3, S6 and S9 as determined by annual band counting. Also shown are U/Th age determinations (black dots with error bars).

Table 1
Stalagmite S3 and S9 uranium and thorium isotope concentrations and calculated ages

Sample	Depth		Concentration ^{238}U		Concentration ^{232}Th		Concentration ^{230}Th		$\delta^{234}U$		Age uncorrected		Age (detritus corrected)[a]	
	(cm)	± (cm)	(ng/g)	± (ng/g)	(pg/g)	± (pg/g)	(fg/g)	± (fg/g)	(‰)	± (‰)	(yr BP)	± (yr BP)	(yr BP)	± (yr BP)
S3[b]	3.1	0.3	292.8	0.7	205.64	3.4	9.4	2.1	32.9	5.7	210	45	190	41
S3[b]	8.8	0.3	310.8	0.7	827.29	7.9	41.3	1.8	42.5	4.6	860	40	780	36
S3[b]	14	0.3	274.4	1.0	2446.4	38.0	95.0	6.2	26.5	8.8	2280	170	2030	151
S3	14.9	0.3	279.2	0.7	413.8	5.4	19.8	2.7	44.1	3.9	460	60	420	55
S3[b]	18.8	0.3	247.5	0.6	859.1	7.1	34.0	1.3	44.2	6.0	890	40	790	36
S3[b]	23.5	0.3	288.3	7.2	583.5	7.1	42.6	2.2	43.3	82.5	950	130	900	123
S3	24.5	0.3	243.2	0.6	318.4	2.6	29.1	0.7	40.9	4.7	780	25	740	24
S3[b]	25	0.3	230.0	0.7	638.0	3.0	37.0	3.0	47.5	7.8	1030	95	960	89
S9	8.9	0.3	209.1	0.5	363.1	9.5	17.4	2.6	40.2	6.4	540	80	490	73
S9	11.1	0.3	233.5	0.4	289.6	2.5	17.9	0.8	38.8	4.1	500	25	470	24
S9	12.5	0.3	223.6	0.5	483.3	5.4	20.2	2.5	33.4	4.4	590	75	530	67
S9[b]	16.3	0.3	202.0	0.4	1024.0	7.9	45.9	1.4	43.4	3.7	1470	50	1330	45

[a] Th/U ages were corrected for detritus following Ivanovich and Harmon (1993) assuming a $^{232}Th/^{238}U$ isotope ratio of 3.8.
[b] Not shown in Fig. 2b.

mass spectrometer. The phosphoric acid extraction was made at 90°C. All calcite values are reported relative to Vienna Pee Dee Belemnite Standard (VPDB), the reproducibility of standard materials is ±0.08‰ (VPDB).

The thickness of annual bands was measured from high-resolution (1200 × 1600 pixels) digital images, which were taken with a high resolution CCD camera from polished sections and thick sections (0.5 mm thick). Multiple counts indicate an error of approximately 1–1.5% of the absolute age.

5. Results

5.1. Chronology

The chronology of all stalagmites is based on both Uranium-series dating and counts of annual growth bands. Uranium-series dating of stalagmites from Kahf Defore is difficult because Uranium contents are low (Table 1) and speleothem calcite contains high amounts of dust, as indicated by high ^{232}Th concentrations. Because the ^{230}Th ion-beams were too small and unstable to measure reliable $^{230}Th/^{229}Th$ ratios, it was not possible to determine ages for material above 150 mm for S3 and 90 mm for S9. Despite these difficulties, we were able to obtain three reliable U/Th-ages out of eight for stalagmite S3 and four for S9.

The depth versus age plot of stalagmite S3 (Fig. 2b) reveals that the number of counted growth bands is in excellent agreement with the two U/Th ages, indicating that S3 grew at a quite constant growth rate beginning at approximately AD 1212. We assign a cumulative age estimate error of approximately ~11 years to our growth band counts down to the year AD 1212. Stalagmite S9, however, shows a mismatch between counted growth bands and measured U/Th ages,

indicating that stalagmite growth ceased between approximately AD 1610 and AD 1765 (Figs. 2a and b). This hiatus appears to be specific only to this sample and may have been caused by a change in the flow path of seepage water or a temporary blockage of the fissure (plumbing). Age calibration of stalagmite S6 is based on annual growth layer counts only, whereas the beginning of growth at 1764 is in excellent agreement with the second growth phase of the nearby stalagmite S9.

5.2. Oxygen isotopic composition of precipitation and cave drip water

Unfortunately, no long-term isotope database for precipitation exists in Southern Oman, but monsoon precipitation samples were collected in 1985 (Clark et al., 1987), 1988 and 1989 (Wushiki, 1991) and 1999 (Fleitmann et al., 1999). The $\delta^{18}O$ values of monsoon precipitation sampled in August 1999 vary between −0.3 and 1.0‰ (VSMOW) and are thus very close to original seawater values, mainly because the precipitation has a very short meteorological history and fractionation effects during evaporation and condensation cancel one another. Fig. 3b reveals that the oxygen isotopic composition of precipitation becomes lighter with altitude (altitude effect). Clark et al. (1987) and own data (Fleitmann et al., 1999) suggest a decrease of 0.15‰ (SMOW) per 100 m rise in elevation (Fig. 3b), whereas Kahf Defore is located at 150 m above sea level and $\delta^{18}O$ values of precipitation typically vary around 0.6‰ (SMOW). Furthermore, Fig. 3c shows that a moderate correlation exists between the amount and $\delta^{18}O$ of monsoon precipitation, with higher monsoon rainfall exhibiting more negative $\delta^{18}O$ values. This inverse relation between the amount and $\delta^{18}O$ signal of precipitation is typically assigned to the so-called "amount effect" (Dansgaard, 1964; Rozanski et al., 1992). The oxygen isotopic composition of cave drip waters sampled in November 1998 and August 1999 vary between 0.87‰ and 1.57‰ (VSMOW) and is only slightly enriched compared to monsoon precipitation, indicating that infiltrating water is not significantly affected by evaporation. This is not surprising, because the high humidity during the monsoon season, caused by the permanent presence of fog, and the rapid infiltration of the water through the thin soil zone minimize the effects of evaporation during the rainy season.

5.3. Stable isotopic composition of present-day and fossil speleothem calcite

The oxygen isotopic composition of actively growing speleothems ranges from −0.57‰ to 1.34‰ (Fig. 4a). The high-resolution $\delta^{18}O$ profiles, their average temporal resolution varies between 1.2 and 1.4 years (Fig. 5), range from −1.51‰ to 0.49‰. All $\delta^{18}O$ profiles show a good correlation in pattern and isotopic range. Solely stalagmite S6 exhibits on average slightly more positive $\delta^{18}O$ values than S3. However, the mean difference in $\delta^{18}O$ between the three stalagmites is within ±0.3‰. All oxygen isotope profiles exhibit distinct decadal-scale oscillations with low amplitude shifts of 0.5 to 1‰. There are four distinct intervals with on average less negative $\delta^{18}O$ values occurring at approximately AD 1307–1631, 1761–1795 (not obvious in S6 record (Fig. 5), 1884–1907 and 1954–1996. The constant trend towards more positive $\delta^{18}O$ values since the 1950s is clearly evident in both the S3 and S6 record. Periods with persistently more negative $\delta^{18}O$ values occur

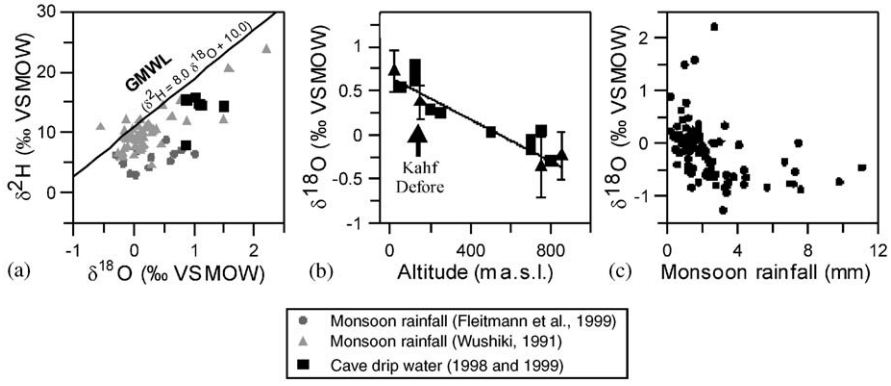

Fig. 3. (a) Isotopic composition of monsoon rainfall in the Dhofar region, sampled in 1989 and 1999 (gray triangles; Wushiki, 1991) and 1999 (gray dots, Fleitmann et al., 1999). Isotopic composition of caves seepage water (black dots; Fleitmann et al., 1999), sampled in 1998 and 1999, is also shown. Black solid line defines the Global Meteoric Water Line (GMWL) (Craig, 1961). (b) Influence of the so-called "altitude effect" on oxygen isotope composition of monsoon rainfall. Black squares are rainfall samples collected in 1999 on transect from the Salalah Plain up to the Dhofar Mountains (see also Fig. 1b). Additionally shown are the isotopic compositions of monsoon rainfall (black triangles) sampled in 1985 (Clark et al., 1987). Vertical error bars are the standard deviation of multiple samples collected at different days. (c) Correlation between $\delta^{18}O$ and amount of monsoon rainfall (sampled 1988 and 1989; Wushiki, 1991).

between AD 1230–1307, 1631–1760, 1820–1860, and 1907–1954 (Fig. 5).

5.4. Annual growth band thickness

Annual bands are couplets of a dense and porous layer. Mean annual band thickness varies between 0.35 (S3; Fig. 5b), 0.30 (S6; not shown) and 0.33 mm (S9; not shown), generally varying between 0.11 and 0.76 mm. The growth rate never exceeds the estimated maximum limit of 1 mm yr^{-1} for calcium concentrations of 0.5 to 2.6 mmol l^{-1} (Dreybrodt, 1980; Baker and Smart, 1995). Drip waters in Kahf Defore have an average Ca^{2+} concentration of 0.9 mmol l^{-1} ($n=3$; unpublished data).

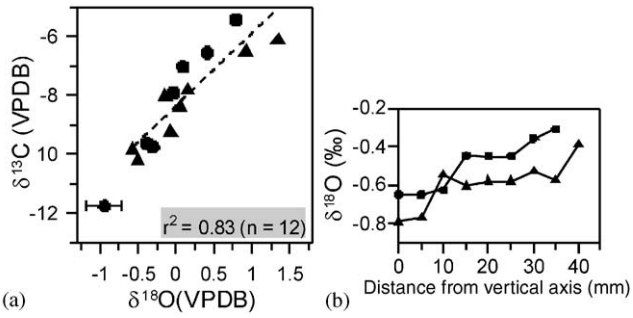

Fig. 4. (a) Oxygen and carbon isotopic composition of modern stalagmites (black dots) and stalactites (black triangles) from Kahf Defore. Black dot with error bar indicate calculated $\delta^{18}O$ of calcite precipitating in isotopic equilibrium with cave cave drip water at 25 ± 0.5°C. (b) $\delta^{18}O$ variations along a single growth layer (''Hendy-test'', Hendy, 1971).

6. Discussion

6.1. Palaeoclimatic significance of $\delta^{18}O$

Whether the studied stalagmites were deposited in isotopic equilibrium is of crucial importance for speleothem-based palaeoclimate reconstructions. Kinetic fractionation processes, such as kinetic loss of carbon dioxide and evaporation of water, can seriously affect the isotopic composition of speleothem and, thus, blur the climatic signal. This might be especially the case for caves located in arid and semi-arid areas, such as Kahf Defore. One robust test for isotopic equilibrium is to use $\delta^{18}O$ of modern seepage water and to calculate expected $\delta^{18}O$ of stalagmites growing in isotopic equilibrium using the temperature-dependent fractionation of ^{18}O between water and calcite (O'Neil et al., 1969). If calculated $\delta^{18}O$ values are in agreement with those of actively growing stalagmites then stalagmites grow in isotopic equilibrium. This test indicates that $\delta^{18}O$ values of actively growing stalagmites, ranging from −0.57‰ and 1.34‰, are slightly enriched with respect to expected values for isotopic equilibrium with measured cave drip waters (Fig. 4a). An additional evidence for non-equilibrium deposition is a progressive increase of $\delta^{18}O$ along a single growth band (the so-called ''Hendy''-test, Hendy, 1971; Fig. 4b). Two profiles along a single growth band, shown in Fig. 4b, clearly reveal a slight increase of 0.3–0.4‰ in $\delta^{18}O$ out of the growth axis. Both tests clearly reveal, that stalagmites from Kahf Defore do not grow in perfect isotopic equilibrium with its parent drip waters, because the relative humidity of <98% and very low drip rates (generally less than 1 drip per minute) favor evaporation and thus kinetic fractionation. Despite the common prejudice that stable isotope profiles of stalagmites affected by kinetic fractionation are not suitable for paleoenvironmental reconstructions (Hendy, 1971; Schwarcz, 1986), we suggest that $\delta^{18}O$ values of our stalagmites from Kahf Defore can be used as a proxy for the amount of rainfall for the following reasons.

Firstly, $\delta^{18}O$ values of speleothem calcite mainly reflect changes in $\delta^{18}O$ of cave drip water and rainfall respectively rather than temperature. If $\delta^{18}O$ would be solely temperature-controlled, then the overall range of measured $\delta^{18}O$ values (1.7‰) would require more than 7°C of variation in average annual temperature, much too large to be reasonable. Nor is the isotopic composition of rainfall related to temperature in the tropics. Rather, in the tropics the oxygen isotopic composition of rainfall is inversely related to the amount of rainfall (see also Figs. 3c and 5). This so-called ''amount effect'' is best developed in tropical and subtropical areas, such as Southern Oman, where the mean annual temperature exceeds 15°C (Dansgaard, 1964; Rozanski et al., 1992). Thus, more negative stalagmite $\delta^{18}O$ values reflect higher monsoon rainfall and vice versa.

Secondly, our interpretation that more negative $\delta^{18}O$ values are an indicator for the amount of rainfall is strongly supported by measurements of the thickness of annual growth bands. As mentioned before, numerous studies have shown that speleothem growth and the thickness of annual bands correlate positively with the quantity of drip water supply, which, on the other hand, relates to the amount of surface rainfall (e.g. Genty and Quinif, 1996; Holmgren et al., 1999; Polyak and Asmeron, 2001). The environmental settings in Kahf Defore strongly support our assumption that thicker annual bands relate to the amount of surface rainfall, because the cave has a short hydrological connection to the surface, there is little, fissured overlying bedrock and from there cave drip rates should respond rapidly to changes in surface rainfall. Furthermore, rainfall in Southern Oman is highly seasonal, more than 80% of rainfall occurs from July to September. Therefore, it is very likely that band thickness is moisture limited, whereas thicker annual bands indicate higher amount of

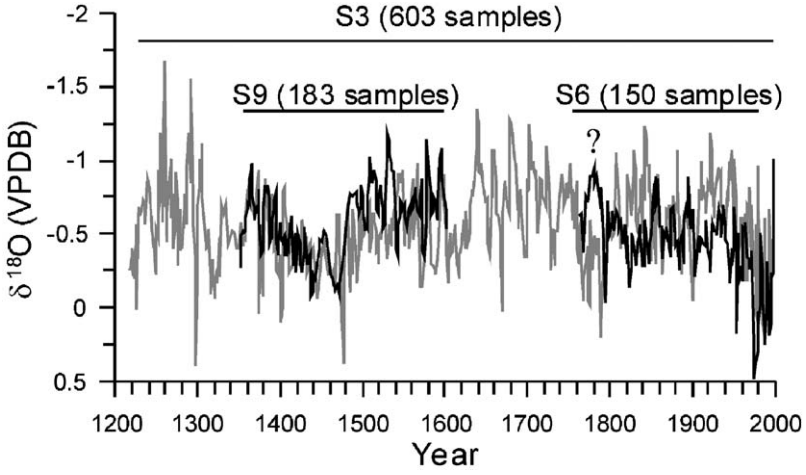

Fig. 5. Comparison of the $\delta^{18}O$ of stalagmites S3, S6 and S9.

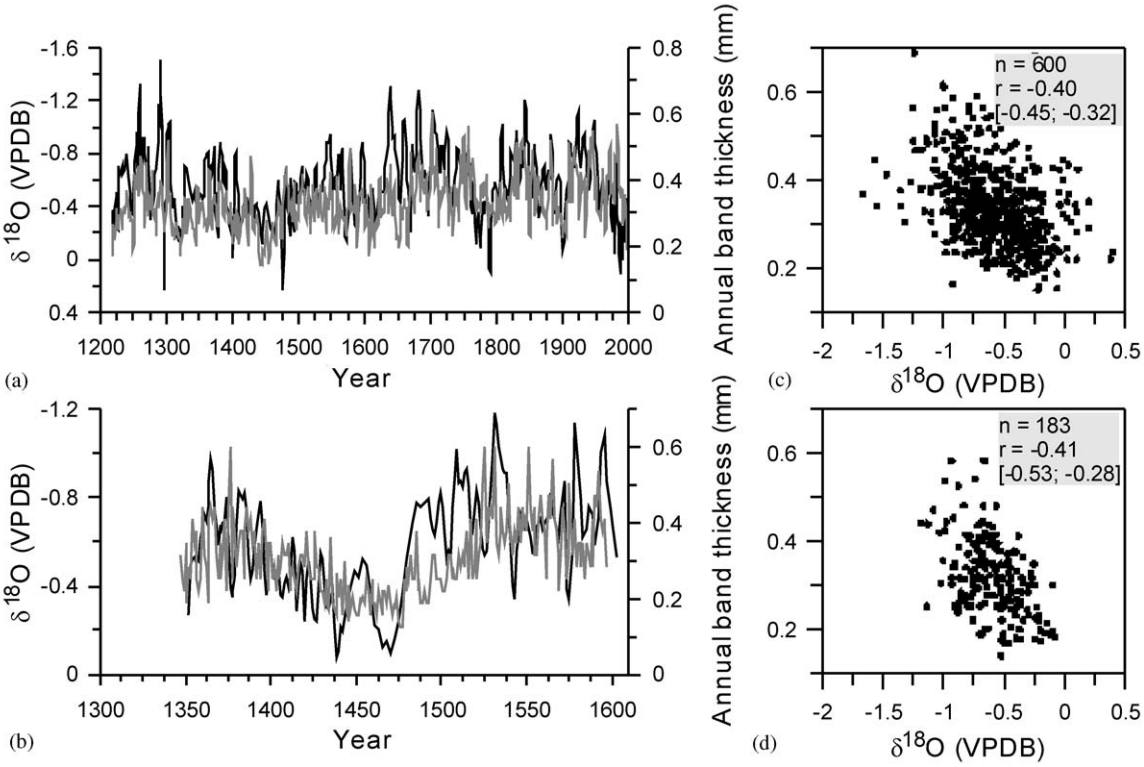

Fig. 6. $\delta^{18}O$ and annual band thickness profiles for stalagmite S3 (a) and S9 (b) correlation analysis for $\delta^{18}O$ and annual band thickness for stalagmite S3 (c) and S9 (b). *n* is the number of data points, *r* is Perason's correlation coefficient, and *P* is the probability that two uncorrelated time series would exhibit a correlation higher in absolute value (Mudelsee, 2003).

monsoon rainfall. The visible and statistically significant negative correlation of $r = -0.40$ and -0.41 between $\delta^{18}O$ and annual band thickness for stalagmites S3 and S9 strongly support our assumption that both proxies reflect the amount of rainfall (Figs. 6a–d). In this case, thicker annual growth bands correlate with more negative $\delta^{18}O$ values and vice versa.

Thirdly, additional processes, such as changes in evaporation in the soil zone, humidity within the cave and the degree of kinetic fractionation associated with changes in the drip rate, might also cause variations in the $\delta^{18}O$ signal. However, all these processes act in the same "direction" as the amount effect. For instance higher monsoon rainfall leads to reduced evaporation in

the soil zone, higher drip rate and higher relative humidity within the cave, leading to thicker growth bands and more negative $\delta^{18}O$ values.

Thus, our overall interpretation is that $\delta^{18}O$ and annual band thickness reflect fluctuations in effective moisture and monsoonal rainfall, respectively. The modern climate conditions in Southern Oman, with the strong seasonality of rainfall and one source of moisture (Indian Ocean), greatly facilitate our interpretation. Finally, the fairly good correlation between the stable isotope profiles of contemporaneously deposited stalagmites clearly reveals that sample specific noise does not blur the climatic signal (Fig. 5).

Finally, the question remains whether our speleothem-based time series reflect local or broader regional rainfall variability. To answer this question, we compared the S3 $\delta^{18}O$ record with two time series of gridded annual rainfall anomalies (Vose et al., 1992; Hulme, 1996; Fig. 7). Although individual anomalies are not always correlated, all records clearly reveal a decrease in monsoon precipitation since the 1960s. Ensuing from the similarity between all records, we suggest that stalagmites from Oman are suitable recorders of rainfall variability on decadal timescales over a broad region.

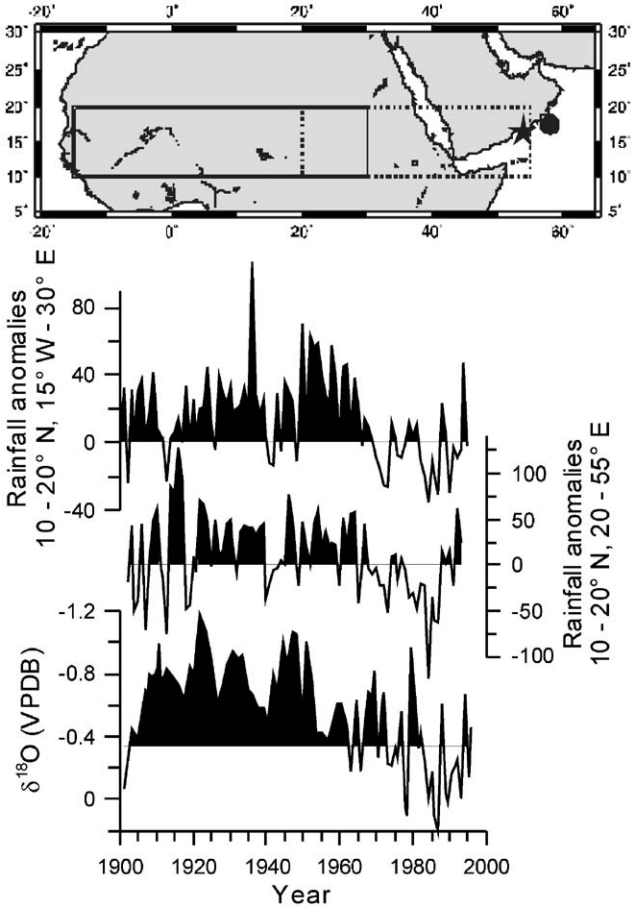

Fig. 7. Comparison of S3 $\delta^{18}O$ (black star) with instrumental rainfall records from Northern Africa (solid black line, Hulme, 1996) and from East Africa and southern Arabia (dashed black line; Vose et al., 1992). Black coloured indicate rainfall above the 1961–1990 average. Note that the number of meteorological stations decreases over time. Black dot shows location of two marine sediment cores (Anderson et al., 2002), which are shown as a composite record in Fig. 8.

6.2. Indian Ocean monsoon rainfall variability during the last 780 years

Although the S3 record shows no long-term trend, there occur distinct high-amplitude decadal and multi-decadal fluctuations in monsoon rainfall. The transition from the Medieval Warm Period (MWP) to the Little Ice Age (LIA) occurs at approximately AD 1310 and is indicated by a sharp and significant reduction in monsoon rainfall, as indicated by a distinct shift to more positive $\delta^{18}O$ values (Fig. 8). Although the LIA is recorded in many continental temperature records (e.g. Mann et al., 1998), a considerable scatter in timing and duration exists. Similarly no agreement upon the end of the LIA exists and it has been variably listed as AD 1700, 1850 or 1900 (Lamb, 1977). The S3 $\delta^{18}O$ profile reveals, supported by the partly overlapping S9 $\delta^{18}O$ profile (Fig. 5), that monsoon rainfall was almost persistently low between AD 1310 and 1660, with lowest rainfall occurring between AD 1450 and 1480. This interval corresponds to the coldest three decades (AD 1449–1478) in the mean annual temperature reconstructions for the Northern Hemisphere (Mann et al., 1998; Bradley, 2000). This link between cooler Northern Hemisphere temperature and the Indian monsoon may reveal that periods with on average cooler temperatures and expanded snow cover over Eurasia weakened monsoon strength and monsoon rainfall, respectively

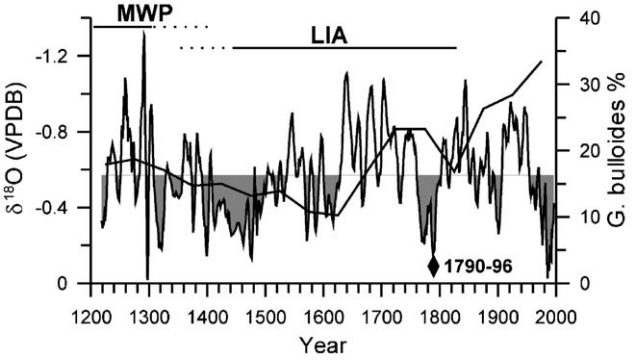

Fig. 8. Comparison of S3 $\delta^{18}O$ (smoothed using a 5-point weighted average) with a marine upwelling (expressed as abundances of *G. bulloides* in percent) record offshore Oman (bold black line). Gray shaded area indicates above long-term average $\delta^{18}O$ values. Bold black lines above the graphs show the estimated extent of the Medieval Warm Period (MWP) and the Little Ice Age (LIA), based on the S3 record. Black diamond indicates the prolonged 1790–1796 El Niño event (Quinn, 1992).

(Barnett et al., 1988). After AD 1660 monsoon rainfall was almost entirely above the long-term average, indicating that the LIA was a relatively short lived period in Southern Oman. Supporting evidence for a relatively short LIA comes from a marine record offshore Oman (cores RC2735, 18°N 14′N; 57° 36′E and RC2730, 18° 13′N, 57° 41′E; Anderson et al., 2002; see Fig. 7 for sampling location), where a rise in the abundance (expressed as percentage of 41 species) of the foraminifer *Globigerina bulloides* starts at approximately AD 1630 and indicates an increase in monsoon wind strength (Fig. 8). Higher abundances of *G. bulloides* are interpreted to indicate increased upwelling of cold deepwater due to stronger summer monsoon winds. Monsoon rainfall was generally high between AD 1660 and 1760. A period of strongly reduced monsoon rainfall occurred between ~AD 1760 and 1800, with a distinct minimum in monsoon rainfall between ~AD 1790 and 1800. This distinct period of decreased monsoon rainfall in Southern Oman coincide with the prolonged 1789–1793 El Niño event, low Nile river discharge (Quinn, 1992) and a period of serious droughts that caused 600,000 deaths in India (Grove, 1998). From AD 1800 to 1950 monsoon rainfall was almost persistently above the long-term average, coinciding with strong monsoon winds over the Arabian Sea (Anderson et al., 2002). A relatively short 20 yearlong interval of reduced rainfall occurred between AD 1880 and 1900. Since AD 1960 monsoon rainfall continuously decreased in Southern Oman, with a minimum in monsoon rainfall in the mid 1980s (Figs. 7 and 8). In contrast, the Arabian Sea upwelling record offshore Oman documents a strong increase in monsoon wind strength. Anderson et al. (2002) suggested that the strong warming of Eurasia during the last decades strengthened the land–sea temperature contrast and, thus, the pressure gradient that drives the Indian monsoon. As a result of the stronger pressure gradient, monsoon wind speed increased and upwelling of cold water in the Arabian Sea was intensified, as indicated by higher abundances of *G. bulloides*. Consequently, one would expect that increased monsoon wind speed, due to a stronger land-sea temperature contrast, go along with increased monsoon rainfall. However, neither meteorological rainfall data from the Sahel zone in Africa (Vose et al., 1992; Hulme, 1996; Fig. 7) and India (Parthasarathy et al., 1994, not shown) nor our speleothem data from Southern Oman indicate such a concurrent increase in monsoon rainfall. Rather, these records show that monsoon rainfall decreased (Meehl and Washington (1993), Parthasarathy et al. (1994), Hulme (1996) and Burns et al. (2002); see also Fig. 7) during the last three decades. Meehl and Washington (1993) suggested by examining observed surface air temperature anomalies after the post-World War II era that the land-sea temperature contrast rather decreased and monsoon performance weakened because the overall warming was greater over the Indian Ocean than over the land from 1971 to 1990 (an absolute increase of 0.28°C over the Ocean versus 0.07°C over land). However, the apparent inconsistency between a few well-constrained terrestrial and marine proxy records underlines the necessity of additional geographically well-distributed long-term proxy records, such as coral records, from the Indian Ocean monsoon domain. Solely a dense network of observations will help to complete the Indian Ocean monsoon "puzzle"

7. Summary

Three annually laminated stalagmites from Kahf Defore in Southern Oman provide a millennial long and annually resolved record of Indian Ocean monsoon variability, which helps to fill the lack of historical climate records in Southern Arabia. The study of the active water-carbonate system in Kahf Defore clearly reveals that modern stalagmites do not grow in isotopic equilibrium and that $\delta^{18}O$ calcite values are affected by evaporation occurring within the cave. However, despite kinetic fractionation $\delta^{18}O$ values can be used for palaeoclimate reconstructions because $\delta^{18}O$ values are inversely related to the amount of precipitation. Supporting evidence for this association derives from the comparison with an independent rainfall related proxy. Thickness of annual growth bands shows a good correlation with $\delta^{18}O$ values, where thicker growth bands correlate with more negative $\delta^{18}O$ (higher rainfall). The striking similarity of overlapping $\delta^{18}O$ time series derived from contemporaneous deposited stalagmites reveal that the signal to noise ratio is, despite kinetic fraction, high. This study shows that stable isotope profiles of stalagmites affected by kinetic fractionation can be used for palaeoclimate studies. Finally, the comparison with instrumental rainfall records from Northern Africa and Southern Arabia shows similar climatic trends over the last 100 years and reveals that the speleothem records from Southern Oman reflect climate variability over a broader region.

The longest stalagmite record clearly shows the transition at AD 1320 from a generally wetter Medieval Warm Period to a drier Little Ice Age, which was of short duration in Southern Oman (AD 1320–1660). Monsoon precipitation decreased since the 1960s, which is also seen in meteorological records throughout Northern Africa. The decrease in monsoon intensity is related to increasing sea surface temperatures in the Southern Indian Ocean, which exceeded warming of Eurasia since 1971. However, our records also reveal that this decrease in monsoon intensity is not outside the range of the past eight centuries.

References

Agnihotri, R., Dutta, K., Bhusan, R., Somayajulu, B.L.K., 2002. Evidence for solar forcing on the Indian monsoon during the last millennium. Earth and Planetary Science Letters 198, 521–527.

Anderson, D.M., Overpeck, J.T., Gupta, A.K., 2002. Increase in the Asian southwest monsoon during the past four centuries. Science 297, 596–599.

Baker, A., Smart, P.L., 1995. Recent flowstone growth rates: field measurements in comparison to theoretical predictions. Chemical Geology 122, 121–128.

Baker, A., Smart, P.L., Edwards, R.L., Richards, A., 1993. Annual growth bandings in a cave stalagmite. Nature 364, 518–520.

Bar-Matthews, M., Ayalon, A., Mattews, A., Sass, E., Halicz, L., 1996. Carbon and oxygen isotope study of the active water-carbonate system in a karstic Mediterranean cave: implications for palaeoclimate research in semiarid regions. Geochimica et Cosmochimica Acta 60, 337–347.

Barnett, T.P., Dumenil, L., Schlese, U., Roekler, E., Latif, M., 1988. The effect of Eurasian snow cover on regional and global climate variations. Journal Atmospheric Science 46, 661–685.

Bradley, R.S., 2000. Past global changes and their significance for the future. In: Alverson, K.D., Oldfield, F., Bradley, R.S. (Eds.), Past Global Changes and their Significance for the Future. Quaternary Science Reviews 19, 391–403.

Bräuning, A., 1994. Dendrochronology for the last 1400 Years in Eastern Tibet. GeoJournal 34, 75–95.

Burns, S.J., Fleitmann, D., Mudelsee, M., Neff, U., Matter, A., Mangini, A., 2002. A 780-year annually resolved record of Indian Ocean monsoon precipitation from a speleothem from south Oman. Journal of Geophysical Research-Atmospheres 107, art. no. –4434.

Charles, C.D., Hunter, D.E., Fairbanks, R.G., 1997. Interaction between the ENSO and the Asian monsoon in a coral record of the tropical climate. Science 277, 925–928.

Clark, I.D., Fritz, P., Quinn, O.P., Rippon, P.W., Nash, H., bin Ghalib al Said, B., 1987. Modern and fossil groundwater in an arid environment. A look at the hydrogeology of southern Oman. In: Use of Stable Isotopes in Water Resources Development. IAEA Symposium, Vol. 299, March 1987, IAEA, Vienna, pp. 167–187.

Craig, H., 1961. Isotopic variations in meteoric waters. Science 133, 1702–1703.

Dansgaard, W., 1964. Stable isotopes in precipitation. Tellus 16, 436–468.

Dreybrodt, W., 1980. Deposition of calcite from thin films of calcareous solutions and the growth of speleothems. Chemical Geology 29, 89–105.

Fleitmann, D., Burns, S.J., Matter, A., 1999. Stable isotope study of the active water-carbonate system in caves in Oman: a test of applicability to Palaeoclimate studies. EOS Transactions AGU 80 (46), Fall Meeting Supplement, Abstract OS22B-12.

Fleitmann, D., Burns, S.J., Mudelsee, M., Neff, U., Kramers, J., Mangini, A., Matter, A., 2003. Holocene forcing of the Indian monsoon recorded in a stalagmite from Southern Oman. Science 300, 1737–1739.

Frank, N., Braun, M., Hambach, U., Mangini, A., Wagner, G., 2000. Warm period growth of travertine during the last interglaciation in southern Germany. Quaternary Research 54, 38–48.

Genty, D., Quinif, Y., 1996. Annually laminated sequences in the internal structure of some Belgian stalagmites—importance for Paleoclimatology. Journal of Sedimentary Research 66, 275–288.

Grove, R.H., 1998. Global impact of the 1789–93 El Niño. Nature 393, 318–319.

Hendy, C.H., 1971. The isotopic geochemistry of speleothems: the calculations of the effects of different modes of formation on the isotopic composition of speleothems and their applicability as palaeclimate indicators. Geochimica et Cosmochimica Acta 35, 801–824.

Holmgren, K., Karlén, W., Lauritzen, S.E., Lee–Thorp, J.A., Partridge, T.C., Piketh, S., Repinski, P., Stevenson, C., Svanered, O., Tyson, P.D., 1999. A 3000-year high-resolution stalagmite based record of palaeoclimate for northeastern South Africa. The Holocene 9, 295–309.

Hulme, M., 1996. Recent climatic change in the world's drylands. Geophysical Research Letters 23, 61–64.

Ivanovich, M., Harmon, R.S., 1993. Uranium Series Disequilibrium. Applications to Environmental Problems. Clarendon Press, Oxford, 541pp.

Lamb, H.H., 1977. Climate: Present, Past and Future. Vol. 2: Climatic history and the future. Methuen, London; Barnes and Noble, New York, 835pp.

Lauritzen, S.-E., Lundberg, J., 1999. Calibration of the speleothem delta function: an absolute temperature record for the Holocene in northern Norway. The Holocene 9, 659–669.

Mann, M.E., Bradley, R.S., Hughes, M.K., 1998. Global-scale temperature patterns and climate forcing over the past six centuries. Nature 392, 779–787.

Meehl, G.A., Washington, W.M., 1993. South Asian summer monsoon variability in a model with doubled atmospheric carbon dioxide concentration. Science 260, 1101–1104.

Mudelsee, M., 2003. Estimating Pearson's correlation coefficient with bootstrap confidence interval from serially dependent time series. Mathematical Geology, 35, 651–665.

O'Neil, J.R., Clayton, R.N., Mayeda, T.K., 1969. Oxygen isotope fractionation of divalent metal carbonates. Journal of Chemical Physics 30, 5547–5558.

Parthasarathy, B., Munot, A.A., Kothawale, D.R., 1994. All–India monthly and seasonal rainfall series: 1871–1993. Theoretical Applied Climatology 49, 217–224.

Polyak, V.J., Asmeron, Y., 2001. Late Holocene climate and cultural changes in the Southwestern United States. Science 294, 148–151.

Quinn, W.H., 1992. A study of Southern Oscillation-related climatic activity for AD 622–1990 incorporating Nile River flood data. In: Diaz, H.F., Markgraf, V. (Eds.), El Niño, Historical and Palaeoclimatic Aspects of the Southern Oscillation. Cambridge University Press, Cambridge, pp. 119–149.

Qin, X., Tan, M., Liu, T., Wang, X., Li, T., Lu, J., 1999. Spectral analysis of a 1000-year stalagmite lamina-thickness record from Shihua Cavern, Beijing, China, and its climatic significance. The Holocene 9, 689–694.

Rozanski, K., Araguás-Araguás, L., Gonfiantini, R., 1992. Relation between longterm trends of oxygen-18 isotope composition of precipitation and climate. Science 258, 981–985.

Schwarcz, H.P., 1986. Geochronology and isotope geochemistry in speleothems. In: Fritz, P., Fontes, J. (Eds.), Handbook of Environmental Isotope Geochemistry. Elsevier, Amsterdam, pp. 271–303.

Thompson, L.G., Yao, T., Davis, M.E., Henderson, K.A., Mosley-Thompson, E., Lin, P.-N., Beer, J., Synal, H.-A., Cole-dai, J., Bolzan, J.F., 1997. Tropical climate instability: the last glacial cycle from a Qinghai–Tibetan ice core. Science 276, 1821–1825.

von Rad, U., Schaaf, M., Michels, K.H., Schulz, H., Berger, W.H., Sirocko, F., 1999. A 5000-yr record of climate change in varved sediments from the oxygen minimum zone off Pakistan, Northeastern Arabian Sea. Quaternary Research 51, 39–53.

Vose, R.S., Schmoyer, R.L., Steurer, P.M., Peterson, T.C., Heim, R., Karl, T.R., Enscheid, J., 1992. The Global Historical Climatology

Network: long-term monthly temperature precipitation, sea level pressure, and station pressure data. ORNL/CDIAC-53, NDP-041, Carbon Dioxide Inf. Anal. Cent., Oak Ridge National Laboratory, Oak Ridge, TN.

Webster, P.J., Magãna, V.O., Palmer, T.N., Shukla, J., Tomas, R.A., Yanai, M., Yasunari, T., 1998. Monsoons: processes, predictability, and the prospects for prediction. Journal of Geophysical Research 103, 14451–14510.

Wigley, T.M.L., Brown, M.C., 1976. The physics of caves. In: Ford, T.D., Cullingford, C.H.D. (Eds.), The Science of Speleology. Academic Press, London, pp. 329–358.

Wushiki, H., 1991. $^{18}O/^{16}O$ and D/H of the meteoric waters in South Arabia. Mass Spectroscopy 39, 239–250.

Yonge, C.J., Ford, D.C., Gray, J., Schwarcz, H.P., 1985. Stable isotope studies of cave seepage water. Chemical Geology 58, 97–105.